

Effect of sediment supply limitation on bed form development under non-uniform flow conditions

W. B. Rauen, B. Lin & R. A. Falconer

Hydro-environmental Research Centre, School of Engineering, Cardiff University, The Parade, Cardiff CF24 3AA, UK

ABSTRACT: An open channel experimental investigation of ripple development on an initially flat sand bed was conducted under turbulent subcritical non-uniform flow conditions. The hydraulic model used included a narrower upstream channel, a diverging channel and a wider downstream channel. With the amount of sediment that recirculated in the flume system being very small and no sediment feed system being used, the sediment material required for the development of bed forms originated primarily from the eroded bed material in the upstream channel. Depletion of the supply region eventually created a sediment supply-limited condition, concurrently with the ripple dimensions becoming constant prior to the equilibrium stage being reached. Non-uniform flow induced the simultaneous occurrence of bed forms at distinct stages of development throughout the hydraulic model, where 3-D and 2-D ripples and incipient bed forms were recorded.

1 INTRODUCTION

The development of bed forms under a sediment supply-limited condition appears only recently to have been investigated in more detail, such as by Kleinhans et al. (2002) and Bravo-Espinosa et al. (2003) for alluvial flows, and Bastos et al. (2002) for continental shelf flows. The term ‘sediment supply-limited condition’ is used herein to represent ‘a limitation of available, transportable sediment from which the bed forms are moulded’ (Kleinhans et al., 2002). Such a condition can typically occur in a pool-riffle stream or downstream of a hydropower dam (due to upstream sediment deposition), in sand-gravel mixtures (due to bed armouring) or in areas with an exposed bedrock (due to depletion of erodible sediment) – where a relatively thin layer of sediment may occur over a sandstone bed, such as for older rivers. Under this condition, the bed form dimensions, rate of growth and geometric arrangement cannot usually be predicted from the local hydraulics and sediment characteristics, but are partly or completely related to the characteristics of the sediment supply from upstream (Kleinhans et al., 2002).

Published studies that deal with the quantification of ripple development under a sediment supply-limited condition are rare, and only qualitative analyses of the occurring bed forms were found.

Most previous laboratory investigations of the development of bed forms and ripples in particular, have been primarily conducted in straight channels, under steady uniform flow and unlimited sediment supply conditions. Some key contributions from these studies were a better understanding of the stages of bed form development – as summarised by Raudkivi (1997) – and the development of predictive models of the bed form growth (Nikora and Hicks, 1997; Coleman et al., 2005), among others. However, the validity of such findings to varying flow and sediment transport conditions remains to be confirmed. One further challenge is the determination of the time to equilibrium of the bed form dimensions under such variable conditions (Coleman et al., 2005). These questions have been addressed experimentally by the authors and some of the key findings are discussed herein.

The combined effect of the conditions described above related this study, with an element of generality, to conditions often found in the field and where ripples etc form downstream of a non-sedimentary bed. The main aim of the study was to characterise ripple development in the hydraulic model, with sediment supply becoming critically limited during experimentation.

2 EXPERIMENTATION WORK

2.1 Hydraulic system and model

The hydraulic model was installed inside a large flume located in the Hyder Hydraulics Laboratory, at Cardiff School of Engineering. A description of the flume and other experimentation apparatuses was given by Rauhen et al. (2008a).

The hydraulic model is illustrated in Figure 1. It had three main regions, namely an upstream channel, a diverging channel and a downstream channel. A threefold increase in the flow width along the diverging channel allowed for a decrease of the mean flow velocity by a similar magnitude. The model was made of translucent PVC and the height of the model walls was 50 cm throughout. The upstream channel was 3.0 m long and 30 cm wide, and corresponded to the region of $2.0 \text{ m} < x < 5.0 \text{ m}$ in terms of flume coordinates. The downstream channel was 4.0 m long and 90 cm wide, and was located between $11.0 \text{ m} < x < 15.0 \text{ m}$. The diverging channel connected these two sections and was 6.0 m long, spanning from $5.0 \text{ m} < x < 11.0 \text{ m}$. The width of the diverging channel varied linearly in the longitudinal direction, from $B = 30 \text{ cm}$ at $x = 5.0 \text{ m}$ to $B = 90 \text{ cm}$ at $x = 11.0 \text{ m}$, with a 1:10 aspect ratio. Approximately 1 tonne of sand was used to fill the model bed, up to an initial bed level of 10 cm. The flume was filled to an experimental water depth of $H = 30 \text{ cm}$ above the initial sand bed level.

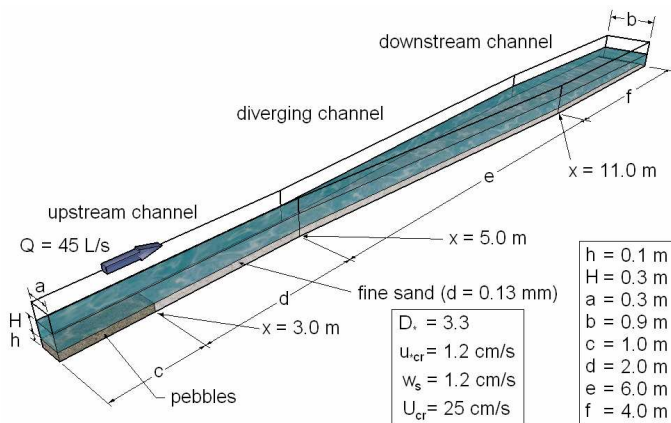


Figure 1 Hydraulic model setup (see text for explanation of parameters)

2.2 Sediment characteristics and erosion threshold

The sediment used in the experiments was fine quartz sand, obtained commercially in washed and graded conditions, with a silica content higher than 98%. The sand was well sorted and uniform, with $d = d_{50} = 130 \mu\text{m}$, where d_{50} is the median grain size.

Some key sediment transport parameters were calculated for the sand used in this study from the formulations of Soulsby (1997), giving $w_s = 1.2 \text{ cm/s}$, $D_* = 3.3$, $\theta_{cr} = 0.065$ and $u_{*cr} = 1.2 \text{ cm/s}$, for the settling velocity, dimensionless grain size, criti-

cal Shields parameter and critical friction velocity respectively. By taking into account the water depth used in the model, the critical mean streamwise velocity for sediment erosion was estimated as $U_{cr} \approx 25 \text{ cm/s}$, using the friction law of Soulsby (1997).

2.3 Experimentation conditions

The flume was first levelled in the horizontal plane for the experiments described herein. A typical experiment would start with a flat sediment bed and, as the experiment progressed, then bed forms would develop under fully turbulent flow conditions, with a constant discharge of $Q = 45 \text{ l/s}$. The values of a number of hydrodynamic and sediment transport parameters estimated for the hydraulic model were obtained using the formulations of Soulsby (1997) and are given in Table 1 and Figure 2.

Table 1 Values of key hydrodynamic and sediment transport parameters estimated for upstream channel ($3.0 \text{ m} < x < 5.0 \text{ m}$)

parameter	value
$U_0 \text{ (m/s)}$	0.50
$Re \text{ (x } 10^3)$	171
Fr	0.29
$u_* \text{ (m/s)}$	0.024
Re_*	2.7
Fr_*	10.9
θ/θ_{cr}	4.0

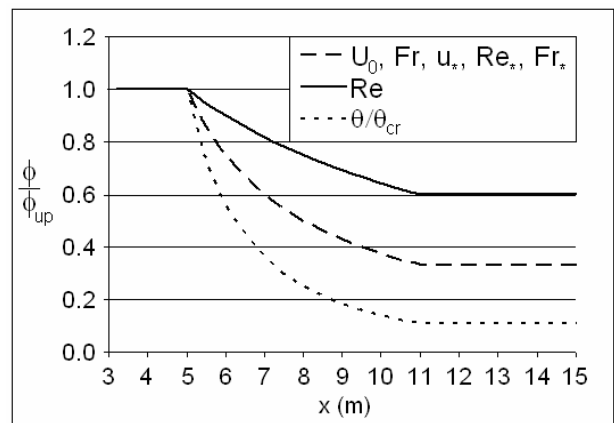


Figure 2 Estimated distributions of hydrodynamic and sediment transport parameters (ϕ) in the hydraulic model, normalised by corresponding values in upstream channel (ϕ_{up})

The cross-sectional mean streamwise velocities were calculated as $U_0 = Q/A$, where A is the cross-sectional area of the flow. The Reynolds and Froude numbers were calculated as $Re = U_0 4R_h/\nu$ and $Fr = U_0/(gH)^{0.5}$ respectively, where ν is the kinematic viscosity, g is gravitational acceleration and R_h is the hydraulic radius. The estimated ranges for these pa-

parameters indicated that turbulent subcritical flow occurred in the hydraulic model.

Several bed profile measurements were undertaken during the experiments to assess bed form development, as outlined below.

2.4 Bed form data acquisition and processing

Bed profile measurements in the hydraulic model were carried out using an Acoustic Doppler probe, i.e. Nortek's Vectrino⁺, operated in sonar mode. The probe was traversed along the x direction centreline. The longitudinal positions and bed elevation values were combined to generate 2-D profiles of the bed. The accuracy of the method, when used under the experimentation conditions reported herein was of the order of 1 mm in the horizontal and vertical directions, when compared against results obtained with a commercial bed profiler equipped with a conductivity probe (see Rauen et al., 2008b for details). Bed profile measurements were carried out at various experimentation times during the transition and final ripple development stages.

The processing of bed profile data involved searching the records for bed surface slopes, so that the slope inflection points along a bed profile could be identified. The bed form height was calculated as the difference in elevation between a trough and the subsequent crest in the upstream direction. Height values not lower than 10d were identified as bed forms and had their height and distance along the x direction recorded.

The most commonly used parameters to describe ripple dimensions are the median and/or the maximum height and length, as reported by several authors. In this study, median ripple heights and lengths, represented by η_{50} and λ_{50} respectively, were calculated at 1.0 m step intervals along the longitudinal direction of the model. The results thus obtained were then associated with the central point of the corresponding intervals. For instance, station $x = 7.0$ m represented the median data calculated between $6.5 \text{ m} < x < 7.5 \text{ m}$, while the data measured in the region of $7.0 \text{ m} < x < 8.0 \text{ m}$ was used to compute the results associated with station $x = 7.5 \text{ m}$, and so forth.

3 RESULTS AND DISCUSSION

3.1 Analysis of bed form development

The measured time variation of the median bed form height and length, i.e. η_{50} and λ_{50} respectively, at

three stations along the hydraulic model channel are shown in Figure 3a and 3b respectively.

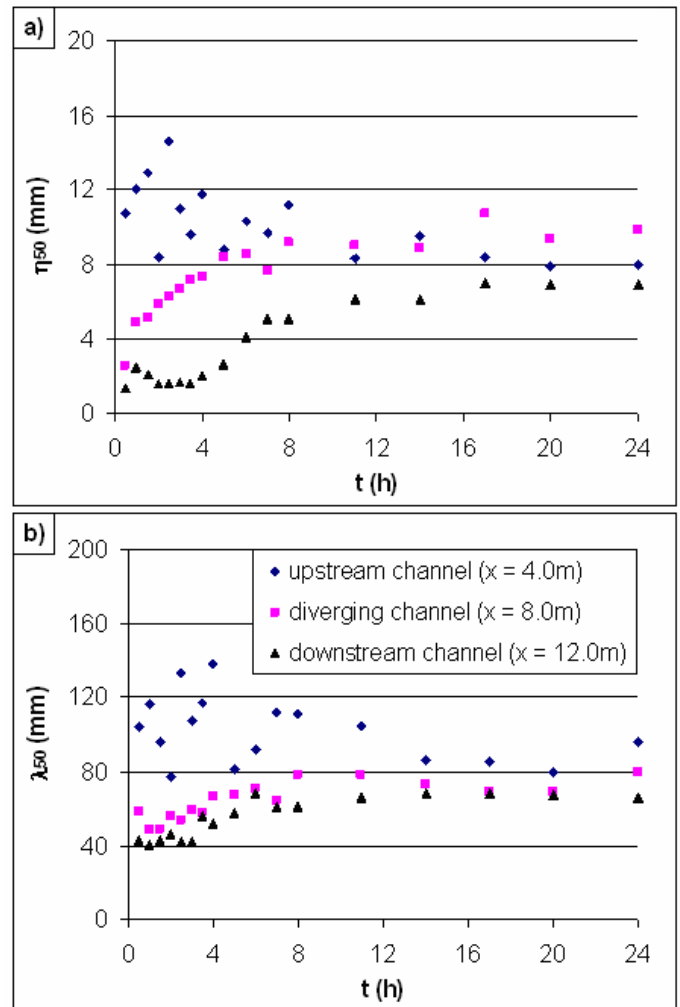


Figure 3 Recorded variations of median bed form dimensions at three sections of the hydraulic model, showing the results for: a) bed form height; and b) bed form length

In general, it can be seen in this figure that three different patterns of bed form development occurred at these stations. In order of increasing θ/θ_{cr} values (see Figure 2), the overall trends were: i) at station $x = 12.0 \text{ m}$, where $\theta/\theta_{cr} < 1$, a trend of increase occurred after a period of approximately constant bed form dimensions (i.e. 4 hr approximately), which then became asymptotic; ii) at station $x = 8.0 \text{ m}$, where $\theta/\theta_{cr} \approx 1$, the ripple dimensions increased monotonically from the start of monitoring, and before tending to an asymptote; and iii) at station $x = 4.0 \text{ m}$, where $\theta/\theta_{cr} \approx 4$, the overall trend was one of reduction of the η_{50} and λ_{50} values after a short period of increase, with a higher scatter in the data for $t < 8 \text{ hr}$ as compared to the rest of the data shown in Figure 3. However, it may be noted that the high data scatter for $x = 4.0 \text{ m}$ probably contained sampling errors due to the 3-D nature of the ripple field in this region (as shown below). The ripple dimensions calculated from the centreline bed profile

measurements may not have represented the ripple crest heights, but included some ripple flanks as well and were therefore probably underestimated (Raudkivi, 1997). In spite of this anomaly, the corresponding bed form dimensions in this region also tended to an asymptote in the end of experimentation.

Key stages of bed form development observed in parts of the hydraulic model are illustrated in Figure 4, where the flow direction was from left to right. Figure 4a depicts the rippled field after 1 hr of experimentation, in the region comprising the end of the upstream channel and the initial part of the diverging channel. The occurrence of 3-D and 2-D ripples in this region can be noted at this time, with a zone of transition from 3-D to 2-D ripples occurring inside the diverging channel. At the end of experimentation, i.e. for $t = 24$ hr, such a zone was typically located near $x \approx 6.5$ m. A higher rate of bed form development was expected to occur in the upstream channel reach as compared with other reaches of the hydraulic model, due to the corresponding values of θ/θ_{cr} being higher. This was confirmed by the observation in that the bed form field evolved quicker in the upstream channel reach in comparison with other regions of the model, following the general sequence from wavelets to 2-D ripples, and then to 3-D ripples (Raudkivi, 1997). In most of the diverging channel reach, the ripple field retained a 2-D character until the end of experimentation, as shown in Figure 4b for the region near $x = 9.0$ m and at $t = 24$ hr.

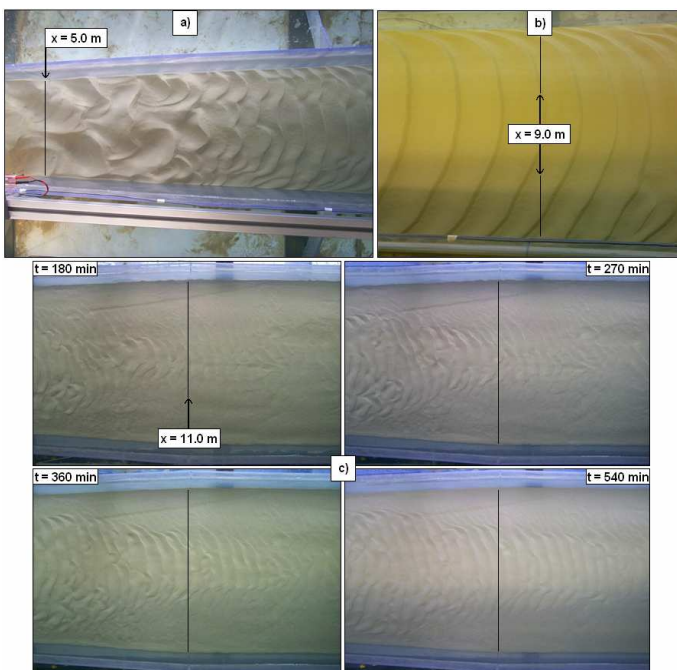


Figure 4 Photographic illustration of bed form development along the hydraulic model, showing the regions located at: a) end of upstream channel and start of diverging channel; b) diverging channel; c) time variation of ripple bed at interface between diverging and downstream channels

Figure 4c illustrates the development of bed forms in the area around the interface between the diverging and downstream channels, i.e. near $x = 11.0$ m, for the experimentation times of $t = 3, 4.5, 6$ and 9 hr. The bed shear stresses in this region were probably considerably lower than the erosion threshold. In spite of this, it can be seen from these photographs that bed form development occurred in this region and was concentrated primarily near the channel centreline. A comparison of the subsequent images in Figure 4c indicated that ripple development was probably induced by an increase in the bed roughness that took place as the upstream ripple field developed, in accordance with the observations of Baas and Best (2000). This phenomenon might also explain the initial period of constant bed form dimensions, as depicted for $x = 12.0$ m in Figure 3, when any bed form induced increase in the bed roughness had not yet been significant enough to initiate bed form development.

An analysis of Figure 4c also indicated that the rate of bed form development near the channel centreline at around $x = 11.0$ m was higher than near the walls, where the bed forms did not appear to develop beyond the incipient stage. Such a non-uniform pattern of bed form development across the channel was probably caused by a non-uniform lateral distribution of the governing hydrodynamic parameters. Therefore, it may be noted that any estimates of ripple dimensions made for the downstream channel, based on the centreline bed profiles, only represented the bed forms along the centreline of the channel.

For the fine sand used in this study, the equilibrium ripple and wavelet dimensions were estimated using empirical equations from the literature. As shown in Table 2, the estimated ranges for the equilibrium ripple height and length were $10 \text{ mm} < \eta_e < 15 \text{ mm}$ and $113 \text{ mm} < \lambda_e < 131 \text{ mm}$ respectively, while the wavelet length and threshold height were calculated as $\lambda_w = 55 \text{ mm}$ and $\eta_w = 7 \text{ mm}$. These estimates are illustrated in Figure 5. Also included in this figure are the final measured bed form dimensions, calculated as the median bed form height and length at each station, time-averaged over the interval of $17 \text{ hr} < t < 24 \text{ hr}$. Such an interval included the last three recorded bed profiles, during the asymptotic period of the bed form development in the model (Rauen et al., 2008c).

It can be noted in Figure 5 that the final bed form height and length values were generally lower than the corresponding equilibrium stage estimates. These results suggested that the bed forms occurring in this study did not reach the equilibrium stage. The subscript 'e' is henceforth used to refer to the final bed

form dimensions occurring in the hydraulic model, as use of the term 'equilibrium dimensions' would be conceptually incorrect in this instance. Furthermore, while the length values were above the predicted wavelet length, the height results for $x > 12.0$ m were below the threshold wavelet height. These results suggested that such bed forms may have remained in the incipient stage during the experiments.

Table 2 Estimated equilibrium ripple and wavelet dimensions for the fine sand of this study (in mm)

Source	η_e	λ_e	η_w	λ_w
Baas (1994)	15	131	---	---
Raudkivi (1997)	15	121	---	55
Soulsby and Whitehouse (2005)	10	129	---	---
Yalin (1985)	---	113	---	---
Rauen et al. (2008a)	---	---	7	---

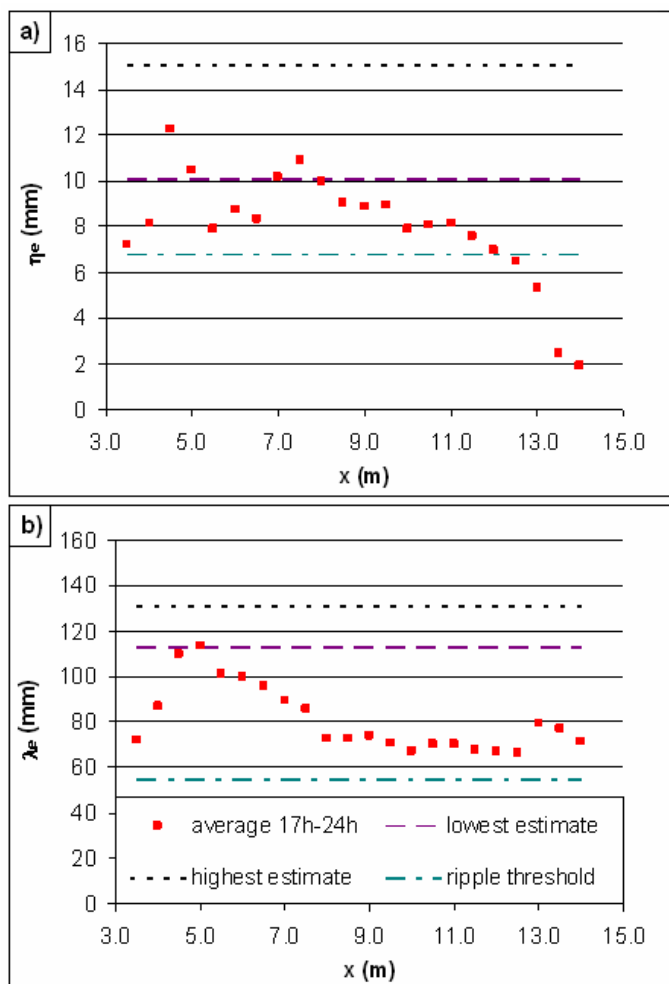


Figure 5 Final bed form dimensions recorded along the hydraulic model, and corresponding estimates of equilibrium ripple and wavelet dimensions, showing the results for: a) bed form height; and b) bed form length

3.2 Characterisation of final bed forms

The above analysis of bed form development, based on measured dimensions and photographic evidence,

led to the conceptual subdivision of the hydraulic model into three main regions, in terms of the corresponding types of final bed forms occurring along the channel centreline. Such regions were defined as being: A) zone of 3-D ripples, for $3.5 \text{ m} < x < 6.5 \text{ m}$; B) zone of 2-D ripples, for $6.5 \text{ m} < x < 12.0 \text{ m}$; and C) zone of incipient bed forms, for $12.0 \text{ m} < x < 14.0 \text{ m}$. A similar scenario, in which a range of bed forms occurred within an overall framework of limited sediment supply, was reported by Bastos et al. (2002), for an area which involved exposed bedrock on the seabed. Kleinhans et al. (2002) reported the simultaneous occurrence of different types of bed forms in alluvial and laboratory flows, although this was deemed to be mainly as a consequence of bed armouring in their study, due to a non-homogeneous bed sediment composition. In this study, the diversity of the final bed forms was regarded as being primarily due to the non-uniform flow and sediment supply-limited conditions occurring in the hydraulic model.

3.3 Discussion

A literature survey suggested that a possible explanation for the interrupted development of bed forms prior to the equilibrium stage being reached, as reported above, was the occurrence of a sediment supply-limited condition in the hydraulic model. The rationale behind this hypothesis was that sediment supply was limited by the amount of sand located primarily in the upstream channel bed, where net erosion occurred in the hydraulic model. Once sediment depletion had taken place, and with the suspended sediment concentration recirculating in the flume water being very low, the main supply of sand for the further development of bed forms was cut off and bed form development ceased.

In the hydraulic model runs, sediment depletion of the upstream channel bed occurred after approximately 17 hours of experimentation. The time for the final ripple height and length to occur were determined, on average, as $t_e = 14$ hr and 11 hr respectively, using an asymptote analysis of the ripple dimensions (see Rauen et al., 2008c for details). Such t_e values were considerably lower - typically by one order of magnitude or more - than any estimates made e.g. for the diverging channel using predictive equations for t_e , such as found in Raudkivi (1997) and Coleman et al. (2005). Hence, the similarity between the time values mentioned above strongly suggested that bed form development in the hydraulic model was limited by sediment depletion occurring in the upstream channel bed. The fact that the

dimensions of the bed forms for different stages of development along the hydraulic model became concurrently unchanged (see Figure 3) appeared to confirm this hypothesis.

It may be added that the final ripple dimensions and time cannot currently be estimated for the non-uniform flow and limited sediment supply conditions, such as those considered in this study. Since these parameters are typically involved in empirical models of ripple development, such as given by Nikora and Hicks (1997) and Coleman et al. (2005), the success in predicting ripple development under such conditions currently relies on making an experimental determination of the final ripple dimensions and time. In fact, Rauen et al. (2008c) showed that the model of Coleman et al. (2005) performed well in predicting the rate of ripple development in zone B of the hydraulic model, provided that the parameters mentioned above were accurately determined.

4 CONCLUSIONS

Non-uniform flow caused different patterns of bed form development to occur in the hydraulic model, both in time and space. The final bed form dimensions occurring in this study fell short of the estimated equilibrium ripple dimensions. A photographic analysis confirmed that bed forms occurring in most of the hydraulic model reach did not achieve equilibrium, in spite of their dimensions becoming asymptotic within the experimentation timescale. The final bed form field comprised three distinct zones, including: 3-D and 2-D ripples and incipient bed forms respectively. Such a scenario is not unusual in nature where, due to the unsteady and/or non-uniform flow and sediment transport processes that occur naturally, the bed forms are found in different stages of development and may not reach equilibrium.

The authors plan to undertake further experiments to verify the applicability of the findings reported herein to other sediment grain sizes and with a sediment feed system.

REFERENCES

Baas, J.H., 1994. A Flume Study on the Development and Equilibrium Morphology of Current Ripples in Very Fine Sand. *Sedimentology*, 41, 185–209.
Baas, J.H., Best, J.L., 2000. Ripple Formation Induced by Biogenic Mounds – Comment. *Marine Geology*, 168, 145 – 151.

Bastos, A.C., Kenyon, N.H., Collins, M., 2002. Sedimentary Processes, Bedforms and Facies, Associated with a Coastal Headland: Portland Bill, Southern UK. *Marine Geology*, 187, 235–258.
Bravo-Espinosa, M., Osterkamp, W.R., Lopes, V.L., 2003. Bedload Transport in Alluvial Channels. *Journal of Hydraulic Engineering*, 129 (10), 783–795.
Coleman, S.E., Zhang, M.H., Clunie, T.M., 2005. Sediment–Wave Development in Subcritical Water Flow. *J Hydraulic Engineering*, 131 (2), 106–111.
Kleinans, M.G., Wilbers, A.W.E., de Swaaf, A., van den Berg, J.H., 2002. Sediment Supply–Limited Bedforms in Sand–Gravel Bed Rivers. *J Sedimentary Research*, 72 (5), 629–640.
Nikora, V.I., Hicks, D. M., 1997. Scaling Relationships for Sand Wave Development in Unidirectional Flow. *Journal of Hydraulic Engineering*, 123 (12), 1152–1156.
Raudkivi, A.J., 1997. Ripples on Stream Bed. *J Hydraulic Engineering*, 123 (1), 58–64.
Rauen, W.B., Lin, B., Falconer, R.A., 2008a. Transition from Wavelets to Ripples in a Laboratory Flume with a Diverging Channel. *International Journal of Sediment Research* (in press).
Rauen, W.B., Lin, B., Falconer, R.A., 2008b. Application of an Acoustic Doppler Velocimeter System as a Bed Profiler. *RiverFlow 2008*.
Rauen, W.B., Lin, B., Falconer, R.A., 2008c. Modelling Ripple Development Under Non-Uniform Flow and Sediment Supply-Limited Conditions. *Geomorphology* (submitted).
Soulsby, R.L., 1997. *Dynamics of Marine Sands – a Manual for Practical Applications*. Thomas Telford Publications, London.
Soulsby, R.L., Whitehouse, R.J.S., 2005. Prediction of Ripple Properties in Shelf Seas. Mark 1 Predictor. HR Wallingford Report TR 150, Release 1.1.
Yalin, M.S., 1985. On the Determination of Ripple Geometry. *Journal of Hydraulic Engineering*, 111 (8), 1148–1155.